

Analysis of pumped thermal energy storage using particle media integrated with concentrating solar power

Joshua McTigue^{*} , Zhiwen Ma

National Renewable Energy Laboratory, 15013 Denver West Parkway, Golden, CO 80401, USA

ARTICLE INFO

Handling editor: .

Keywords:

Concentrating solar thermal
Pumped thermal energy storage
Particle thermal energy storage
Long duration energy storage
Carnot Battery

ABSTRACT

Pumped Thermal Energy Storage (PTES) is an electricity storage system that converts electricity into thermal energy which is stored and later transformed back into electricity. Previous work has illustrated that particles have low capital costs and can be operated over a wide range of temperatures. PTES with particle storage achieves higher round-trip efficiency and specific power output than when molten salt thermal energy storage is used.

This article explores hybrid systems that combine PTES with Concentrating Solar Power (CSP). Hybrid systems share the majority of components thereby reducing costs compared to two stand-alone devices. In addition, hybrid systems can provide multiple services (such as renewable power generation and electricity storage services). Using particle thermal storage in these hybrid concepts provides freedom in choosing the design conditions, since a wide range of operating temperatures is allowable, therefore making it possible to identify hybrid system designs that have good performance.

In this article, two concepts for hybrid PTES-CSP are introduced. Thermodynamic models are developed and these are used to evaluate the performance of two hybrid systems. These models account for turbomachinery efficiency, and approach temperature and pressure loss in heat exchangers, as well as other sources of inefficiency, such as motor-generator losses, and air fan power. The “Solar Top-Up” Concept uses CSP to increase the temperature delivered by the charging heat pump. The discharging system uses a topping gas cycle and a bottoming steam cycle to fully exploit the available energy. Using solar heat to increase the maximum temperature from 750 K to 1100 K increases the round-trip efficiency from 41 % to 62 % and the specific work output from 88 kJ/kg to 301 kJ/kg.

The second concept is a “Dual-Mode” device which provides both electricity storage and solar electricity generation with the same set of components. The PTES-mode and CSP-mode performance are optimized at different design values but careful parameter selection leads to good performance of both modes: one design produces PTES round-trip efficiency > 60 %, CSP heat engine efficiency > 40 %, and specific work outputs > 150 kJ/kg (for both cycles), when the particle receiver temperature is > 1200 K and maximum heat pump temperature is 1100 K.

1. Introduction

Long-Duration Energy Storage (LDES) systems can provide a range of services, including load shifting, resource adequacy, frequency regulation, transmission upgrade deferral and congestion relief. Numerous barriers – such as high capital costs, uncertainty around finance, revenue, and policy, and lack of inclusion in planning tools – have prevented widespread deployment of LDES. However, there is growing recognition of the role required for LDES by future grids. For example, a recent report from the US Department of Energy (DOE) suggested that grids

with high quantities of renewables would require 225–460 GW_e of LDES by 2060 [1]. But achieving commercial deployment requires reduced capital costs (45–55 %), increased round-trip efficiency (7–15 %), and significant changes to market and regulatory mechanisms.

Several governments have started to set mandates for LDES capacity. For example, Italy is targeting 9 GW_e of > 8h-duration storage, Germany is holding auctions for 500 MW_e LDES in 2025–2026 [2], while the California Public Utilities Commission is targeting 2 GW_e of LDES: 1 GW_e with > 12 h duration and 1 GW_e for multi-day storage [3]. Meanwhile, the UK National Wealth Fund (previously the UK Infrastructure Bank) led a funding round to secure £300 million for Highview

^{*} Corresponding author.

E-mail address: josh.mctigue@nrel.gov (J. McTigue).

<https://doi.org/10.1016/j.solener.2025.113436>

Received 12 November 2024; Received in revised form 24 February 2025; Accepted 12 March 2025

Available online 25 March 2025

0038-092X/© 2025 The Authors. Published by Elsevier Ltd on behalf of International Solar Energy Society. This is an open access article under the CC BY license (<http://creativecommons.org/licenses/by/4.0/>).

Nomenclature		W	Work, J
<i>Greek letters</i>		w	Specific work, J/kg
η_{RT}	Round-trip efficiency, Equation (1)	<i>Subscripts/Superscripts</i>	
$\eta_{RT,2}$	Second-law round-trip efficiency, Equation (2)	in, out	Inlet, outlet
η_{HE}	Heat engine efficiency, Equation (3)	chg, dis	Charge, discharge
η_p	Polytropic efficiency	solar	Solar
γ	Ratio of specific heat	o	Ambient conditions
ρ	Density, kg/m ³	RT	Round-trip
ΔT	Approach temperature, K	HE	Heat engine
τ	Duration, h	<i>Acronyms</i>	
<i>Roman letters</i>		CB	Carnot Battery
B	Exergy, J	CSP	Concentrating Solar Power
f_p	Pressure loss factor	LCOS	Levelized Cost of Storage
\dot{m}	Mass flow rate, kg/s	LDES	Long Duration Energy Storage
p	Pressure, bar	PFBHX	Pressurized Fluidized Bed Heat Exchanger
Q	Thermal energy, J	PTES	Pumped Thermal Energy Storage
S	Entropy, J/kg.K	sCO ₂	Supercritical Carbon Dioxide
T	Temperature, K	TES	Thermal Energy Storage

Power to develop a 50 MW_e, 300 MWh_e Liquid Air Energy Storage system [4], and the US DOE Office for Clean Energy Demonstrations has a \$505 million LDES portfolio [5].

Pumped Thermal Energy Storage (PTES) is a system that stores electricity using a thermal energy storage medium. Thermal storage media typically have low costs of marginal energy capacity, so PTES is particularly suitable for LDES applications. A variety of PTES concepts exist, since there are multiple ways to convert electricity to heat, to store the thermal energy, and then to convert the thermal energy back to electricity. A typical design will use a heat pump to transfer energy from a cold storage to a hot storage, thus charging the system with electricity. Later, a heat engine generates electricity using the hot storage as the heat source and the cold storage as the heat sink. A report by the International Energy Agency characterized the key attributes and challenges facing PTES deployment. In particular, it noted that PTES has a high potential to efficiently integrate multiple energy sources and sinks in the electrical and heat sectors. The topic of this article are concepts that integrate PTES with a Concentrating Solar Power (CSP) plant.

CSP uses arrays of mirrors to concentrate sunlight onto a receiver in which fluid is heated and used to drive a heat engine. Storing the thermal energy enables electricity delivery to deferred to the evening or high net load periods. Recent CSP developments have included > 8 h storage duration, and can therefore provide similar services to LDES systems. CSP systems face several deployment barriers, including high capital costs, geographical constraints, and issues with molten salt tank leakage.

PTES and CSP systems have several components in common, such as the thermal energy storage, power cycle, heat exchangers, heat rejection systems, generators, and grid connections. Integrating PTES and CSP may confer advantages such as improved efficiency, reduced component cost, increased energy density, or the possibility for the plant to provide several energy management services and therefore 'stack' revenue streams [6]. These advantages must be weighed against the additional complexity of designing, constructing, and operating such a hybrid plant. Furthermore, a hybrid PTES-CSP has more geographical constraints than a stand-alone PTES. There are numerous ways in which these systems can be hybridized, and four categories are:

- (1) Use a heat pump in a CSP system to improve performance or functionality – e.g.:
 - a. Upgrade solar heat to higher temperatures to enable higher energy densities and efficiencies of the discharging system.

- b. Create a cold storage with a refrigerator and generate electricity by running a heat engine between the solar heat and the cold storage.
 - c. Combine both a) and b). This system could also deliver heat and cold to thermal loads [7].
- (2) Support a PTES system with solar heat:
 - a. Increase the temperature of heat delivered by the heat pump with solar heat addition, see [Section 2.2.1](#)
 - b. Simplify the thermal storage system (or reduce storage volumes) by adding solar heat rather than storing energy
 - (3) Share the hot storage which is charged by both CSP and the PTES which can therefore operate somewhat independently, see [Section 2.2.2](#).
 - (4) Co-location of stand-alone systems. A co-located system may benefit from grid infrastructure, permitting, shared operational staff etc.

Previous work investigated the thermodynamic limits of hybrid systems such as 1a-1c and found that these systems have no efficiency advantages when compared with either a stand-alone PTES or a stand-alone CSP system [6]. That is, the maximum efficiency of a hybrid system when considering the total energy input (electricity plus the exergetic value of solar heat) is the same as the maximum efficiency of a standalone PTES. Therefore, to a competitive technology, hybrid PTES-CSP must achieve economic improvements such as by reducing the capital investment (by sharing equipment) or by enabling the plant to earn revenue from different sources (such as renewable electricity generation and electricity storage).

A concept proposed by Benato [8] upgraded the temperature from a heat pump using an electrical heater. The author described how this system could achieve higher temperatures at lower pressure ratios and therefore reduce the capital cost. The electric-to-electric round-trip efficiency was > 9 % for maximum temperatures above 750 °C. The low round-trip efficiency is partly due to the 'unbalanced' storage; the hot storage capacity is increased but the cold storage capacity is not. Therefore, during discharge, the cold storage is depleted before the hot storage and the system has a surplus of energy. This extra hot energy can be exploited by either using it directly in a thermal process, or converting it to electricity using a bottoming power cycle. One study that used an Organic Rankine Cycle estimated an electric-to-electric round-trip efficiency of ~ 47 % with maximum temperatures of over 1000 °C [9].

Additional thermal energy could be provided by CSP rather than an electric heater, as investigated by Petrollese et al. in Ref. [10] who considered an argon-based Joule-Brayton PTES coupled with packed-bed TES. (Argon is a preferable working fluid for packed-bed PTES due to its high ratio of specific heat capacities, while helium is preferable for liquid-storage PTES due to its high conductivity which improves heat transfer [11]. Nitrogen is used here as it still performs well and is relatively inexpensive). The design proposed by Petrollese et al. could operate independently as a PTES, a CSP system, or a hybrid PTES-CSP system where CSP increased the temperature generated by the heat pump. The authors varied the pressure ratio and showed that increasing the pressure ratio increased the second-law round-trip efficiency of the PTES-CSP hybrid: higher pressure ratios effectively reduced the temperature of rejected heat and led to $\eta_{RT,2} > 60\%$ for a maximum solar temperature of 1000 K. In a subsequent work, the same group investigated the performance of this design under variable solar conditions [12].

Other concepts have proposed integrating a PTES into advanced CSP power cycles. For example, supercritical carbon dioxide (sCO₂) recompression cycles use an additional compressor to facilitate efficient recuperation within the cycle [13]. The recompression occurs to gaseous sCO₂ and thus contributes notably to the cycle work input. An innovation proposed Ref. [14], used PTES to generate and store medium-temperature thermal energy in off-peak times. This stored energy is then used to facilitate recuperation rather than using recompressor. A similar concept was described in Ref. [15] for a novel hybrid Rankine-Brayton cycle using a propane working fluid. A heat pump was used to create the thermal energy needed for recuperation, and the proposed concept was found to be feasible in the Spanish electricity market under some scenarios.

In this article, two hybrid PTES-CSP systems are examined:

1. “Solar Top-Up” in which solar heat is used to increase the temperatures that are delivered by PTES charging phase. The system is then discharged via a topping gas cycle and a bottoming steam cycle, to most effectively use all the thermal energy added to the system.
2. “Dual-Mode System” which has two modes of operation: it can provide both renewable power generation (via CSP) and electricity storage services (via PTES). Most components are shared between the two systems thereby reducing costs compared to two stand-alone devices.

A key design feature of the concepts is the use of particle thermal energy storage. Particles have been developed as a storage material [16] and heat transfer material [17] for CSP applications. Silica particles have low capital costs and can be operated over a wide temperature range [18]. The particles are stored in insulated concrete silos and are transferred into the containers using insulated skip hoists adapted from the mining industry [19]. Heat is exchanged between the particles and the power systems by using pressurized fluidized bed heat exchangers (PFBHX) [20]. Previous work has characterized particle properties, developed handling technologies, and considered economic impacts [21].

Electricity storage systems (i.e. PTES) using silica particles are also being developed. For example, the ENDURING project designed particle electric heaters, storage containers, and particle conveyance systems [19,22]. Particles heated to over 1000 °C can then be used as the heat source for an indirectly heated combined gas turbine cycle. The ENDURING system can conceivably achieve round-trip efficiency > 50 % and pathways to a Levelized Cost of Storage (LCOS) of 5 ¢/kWh_e for 100-hour storage duration were proposed [22].

Subsequent work developed PTES concepts with both hot and cold particle thermal energy storage [23]. This concept is comparable with designs that used alternative storage media, such as molten salts [24,25] or packed beds of rocks [26]. The technical and economic performance of particle-PTES and molten-salt PTES were compared in Ref. [27].

These designs use Joule-Brayton cycles, for which increasing the maximum cycle temperature correlates to a higher round-trip efficiency and work output. Liquids for thermal storage have limited operating temperature ranges, for example, nitrate molten salts freeze at ~ 250 °C and decompose at > 560 °C. Alternative salt blends can reach higher temperatures, for example, chloride molten salts are being developed for Generation 3 CSP and operate between 450 °C and 750 °C [28]. Results in Ref. [27] that indicate that particle-PTES and molten-salt-PTES have very similar performance when operated at the same maximum temperature. Particles can be heated to higher temperatures than molten salts in which case both the round-trip efficiency and specific work output is increased significantly. For example, when the maximum temperature is 560 °C, the round-trip efficiency reaches 55 % and specific work reaches 150 kJ/kg. But using particles to reach 827 °C enables round-trip efficiencies greater than 65 % and specific work outputs over 250 kJ/kg. An economic comparison found that the LCOS of particle-PTES is lower than molten-salt-PTES, with values of 0.115 \$/kWh_e and 0.171 \$/kWh_e, respectively, for 10 h discharge. These cost improvements are due to improved round-trip efficiency, and reduced cost of thermal storage and heat exchangers. For LDES applications, particle-PTES outcompetes optimistic cost projections for lithium-ion batteries: for 100 h discharge, the total capital cost of particle-PTES is 38 \$/kWh_e, compared to 100 \$/kWh_e for batteries.

1.1. Contribution of this article

In this article, two novel hybrid PTES-CSP systems are described, and are referred to as the “Solar Top-Up” system and the “Dual-Mode” system. These designs improve the flexibility of CSP systems and increase the possible value streams. An overview of these concepts and additional background is given in Section 2. Thermodynamic models are developed to evaluate the performance of the hybrid systems, as described in Section 3. These models account for turbomachinery efficiency, and approach temperature and pressure loss in the PFBHX, as well as other sources of inefficiency, such as motor-generator losses, and air fan power. The Dual-Mode System also requires the evaluation of the turbomachinery efficiency and pressure ratio at off-design conditions since the CSP system operates over different temperature ratios than the PTES system. Several design variables and design modifications are investigated, such as pressure ratios and maximum temperatures, and results are presented in Section 4. While some factors uniformly improve performance (such as increasing maximum temperatures) some variables result in trade-offs between different objectives. Operational strategies for the two hybrid concepts are discussed. The concepts and framework developed in this article can be used as the basis for future cost and value studies, and the outlook for such systems is discussed in Section 5.

2. Overview of concepts

2.1. Pumped thermal energy storage

Pumped Thermal Energy Storage (PTES) – also referred to as a Carnot Battery – is a grid-scale electricity storage device [29]. Electricity is transformed into thermal energy which is stored and later converted back into electricity using thermodynamic cycles. PTES achieves low marginal costs of energy storage capacity by using low-cost, abundant materials. As described in Section 1, previous research has considered using solid materials (such as rocks in fixed packed beds) and liquids (such as molten salts and thermal oils). Small particles (such as silica sand) may also be used [23] and a schematic showing how particle silos and fluidized bed heat exchangers are integrated into a PTES is shown in Fig. 1 and a corresponding temperature-entropy diagram is presented in Fig. 2.

In this article, the thermodynamic cycles use a working fluid which remains in the gaseous phase throughout operation. Suitable fluids

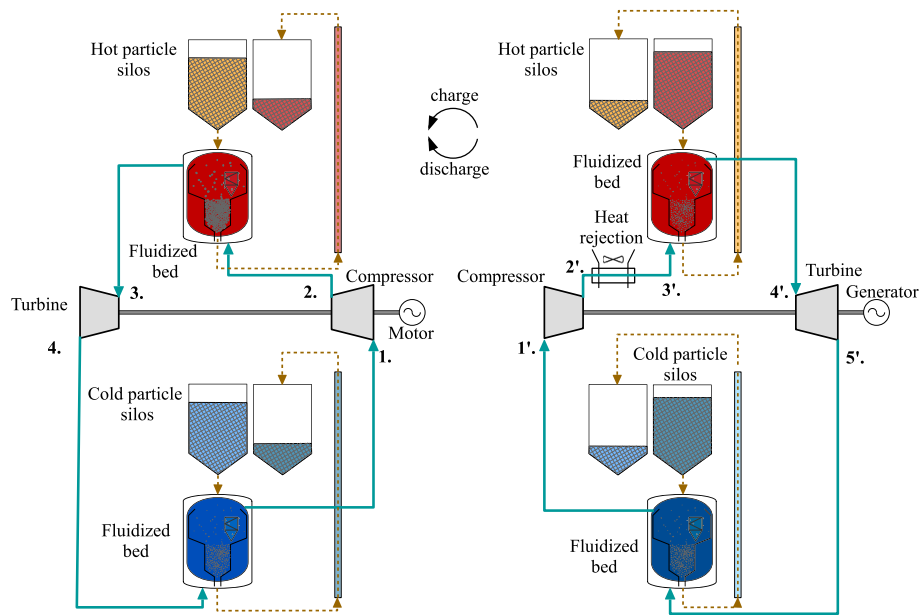


Fig. 1. Schematic of a PTES system using particle storage and PFBHs. The left-hand-side shows the charging heat pump and the right-hand-side shows the discharging heat engine [30].

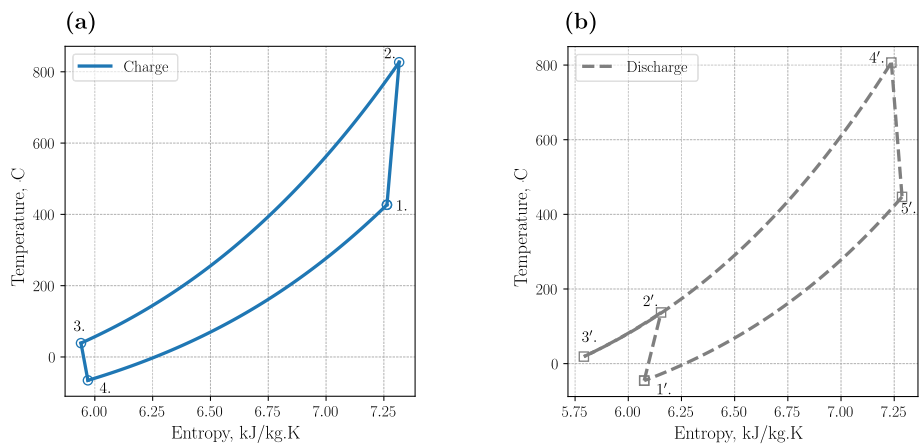


Fig. 2. Temperature-entropy diagram of a nominal PTES system using particle thermal energy storage. Numbering corresponds to Fig. 1. (a) Charging heat pump (b) Discharging heat engine.

include nitrogen, argon, and air, and previous research into PTES using these Joule-Brayton cycles has found that performance is improved by maximizing the temperature difference between the hot and cold storage [31]. Particles may be operated over a larger temperature range than liquid storage. Particles are also stored in unpressurized silos meaning that only the PFBHX requires pressurization. This is advantageous compared to packed-bed storage where pressurized fluids pass through the storage, which therefore requires the storage to be pressurized and increases costs [32]. Another advantage of Joule-Brayton cycles is that the heat capacity of the working fluid does not vary substantially which facilitates heat transfer with sensible storage materials as heat exchanger temperature profiles are “well-matched” and pinch points are likely to be manageable. Furthermore, by using closed cycles with ideal gases, off-design operating points may be managed using inventory control and research has indicated that the system can be operated at part load without significantly compromising the system efficiency [33–35].

A heat pump is used in the charging phase, as shown in Fig. 1a and Fig. 2a. Electrical energy is used to move energy from a heat source (in this case, the cold storage) to the heat sink (the hot storage). This is

achieved with a reverse Joule-Brayton cycle in which gas is first compressed from temperature T_1 to T_2 . Thermal energy is extracted from the gas by cooling it to T_3 with particles in the PFBHX. Particles are removed from a lower-temperature hot silo, heated in the PFBHX, and then deposited in a higher-temperature hot silo. The gas then enters a turbine and is expanded to low pressure and temperature T_4 . The gas is returned to its original temperature T_1 in a second PFBHX in which particles are cooled. Particles are removed from a higher-temperature cold silo, cooled in the PFBHX, and then deposited in a lower-temperature cold silo. For the example shown in Fig. 2, the ‘cold’ storage particles operate between a sub-ambient temperature (~ -45 °C) and a hot temperature (~ 450 °C), whereas the hot storage particles operate between 25 °C and 800 °C.

In the discharging phase, the cycle direction is reversed, so that power is generated from the temperature difference between the hot and cold storage. While the same heat exchangers are used, an additional set of turbomachinery is required (although reversing turbomachinery designs are being developed [36]). The pressure ratio of the discharging cycle is chosen to ensure that both the hot and cold particles are returned to their original temperatures. As a result, the discharging pressure ratio

is larger than the charging pressure ratio [24].

PTES performance is typically judged in terms of the round-trip efficiency η_{RT} ; simply defined as the fraction of input electricity that is recovered during discharge:

$$\eta_{RT} = \frac{W_{out}^{dis}}{W_{in}^{chg}} \quad (1)$$

where W_{in}^{chg} is the net electrical input to the heat pump during charge and W_{out}^{dis} is the net electrical work output during discharge. The specific work output w_{out}^{dis} [J/kg] is also an important parameter because it relates to the investment cost in turbomachinery.

2.2. Hybrid CSP PTES systems

Two hybrid concepts that potentially reduce cost and increase value are described in more detail here and are based on a Category 2 system ("Solar Top-Up Cycle") and a Category 3 system ("Dual-Mode Cycle").

2.2.1. Solar Top-Up cycle

Existing heat pumps typically operate at less than 150 °C although this is historically has been due to a lack of a market for higher temperatures. Compressors in gas turbines output gas in the range of 300–600 °C which indicates what temperatures a high-temperature heat pump using an existing gas compressor could reach. Previous work has shown that Joule-Brayton PTES round-trip efficiency is improved by maximizing the temperature difference between the hot and cold storage [24,26,31], due to increasing the heat engine efficiency at the expense of reducing the heat pump Coefficient of Performance. Deployed CSP systems generate temperatures at 565 °C and higher temperatures in excess of 1000 °C are possible using heliostats and power towers. CSP provides one way to increase the temperature of the hot thermal storage without requiring the development of new heat pump compressor technology.

A hybrid PTES-CSP system which uses CSP to top up the thermal

energy generated by a heat pump is illustrated in Fig. 3. The charging cycle operates in a similar way to the PTES heat pump in Fig. 1a, except that after the hot PFBHX, the hot particles are heated further in a particle receiver by solar irradiance. Cold particle storage is also created by the heat pump. Compared to the PTES concept, the energy capacity of the hot storage has been increased and no longer 'balances' the energy content of the cold storage. Therefore, the discharging system uses both a gas turbine and a bottoming steam turbine cycle exploit excess thermal energy. To discharge the system, a Brayton heat engine extracts power from between the hot and cold storage. This waste heat is available at relatively high temperatures and is used to power a bottoming steam cycle, as shown in Fig. 3.

Fully charging this system requires both the heat pump and CSP system to have operated – i.e. electricity prices and solar availability have to be favorable for both of the systems to charge. This may not be a problem in locations with high penetration of solar photovoltaics, such as California, where low electricity prices coincide with high solar availability. The heat pump and CSP do not have to operate simultaneously but could charge at different times as long as the partially-heated particles can be stored. However, the heat pump must operate first to create the right inlet temperature for the CSP field. When discharging the system, the Joule-Brayton heat engine and steam cycle can operate simultaneously to create a larger power output compared to what a standalone PTES could achieve. It is also possible to add dispatch flexibility by storing the Brayton cycle waste heat and operating the steam cycle at another time.

The round-trip efficiency definition in Equation (1) is modified for hybrid cycles to account for the exergetic value (available work) of the solar thermal energy ΔB_s , so that the second-law round-trip efficiency $\eta_{RT,2}$ is given by

$$\eta_{RT,2} = \frac{W_{out}^{dis}}{W_{in}^{chg} + \Delta B_{solar}} \quad (2)$$

Where $\Delta B_{solar} = \Delta Q_{solar} - T_o \Delta S_{solar}$, in which ΔQ_{solar} is the solar heat addition, ΔS_{solar} is the entropy change, and T_o is the ambient tempera-

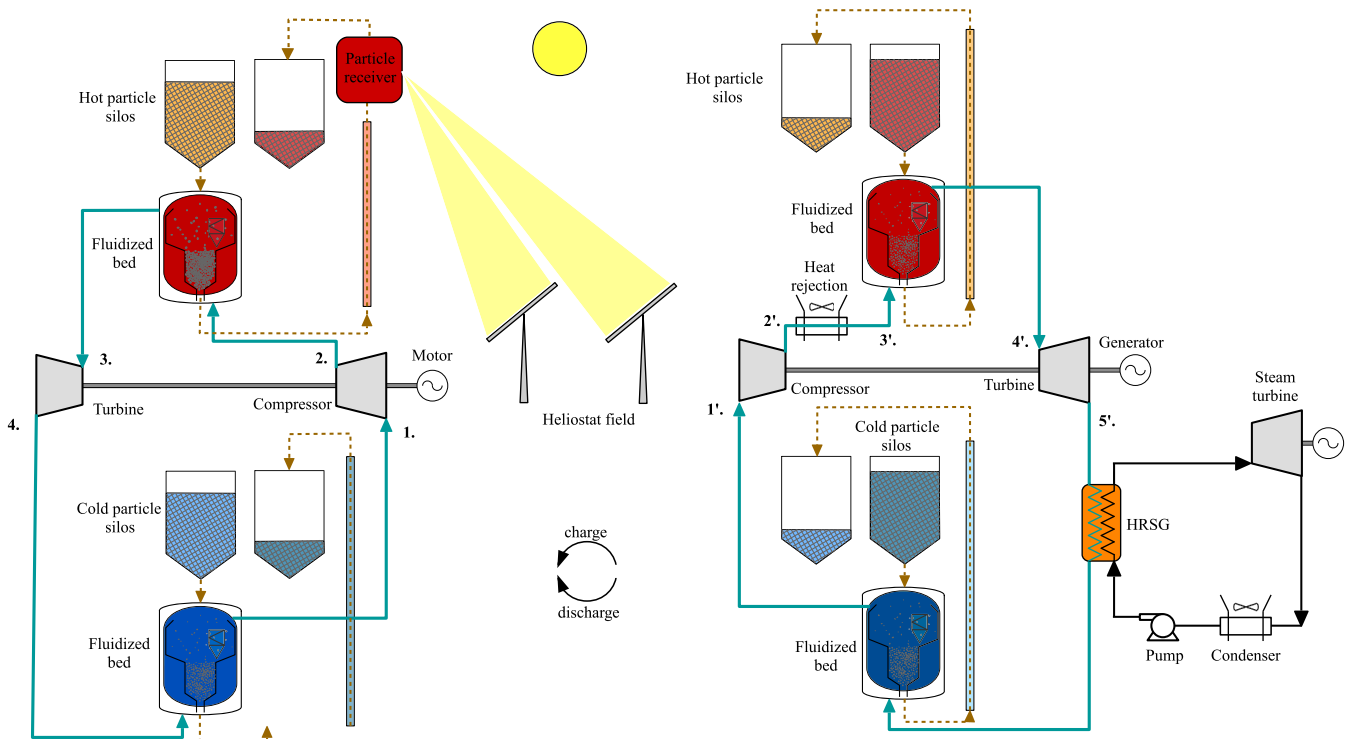


Fig. 3. Schematic of the solar top-up hybrid cycle. (left) During charge, particles are first heated by a heat pump and then solar heat. (right) The discharge cycle includes a bottoming steam Rankine cycle to make use of excess heat.

ture.

2.2.2. Dual-Mode hybrid cycle

The objective of this configuration is to design a system that can operate independently as PTES or a CSP system while sharing several components. Such a system can operate flexibly at reduced cost compared to independent stand-alone systems.

If the CSP and PTES both deliver the same maximum temperature, then the hot thermal storage can be shared between the systems, providing there is sufficient storage capacity. When the hot storage has been charged by the PTES, then a cold storage will have been created, and the system can discharge as a conventional particle-PTES illustrated in Fig. 1. When the system has been charged by CSP, only hot storage is available. While this could be used to power a conventional CSP power cycle (such as a steam cycle), the PTES heat engine can be configured to operate using only hot storage meaning that the same heat exchangers, compressors, and turbines are shared between CSP discharging mode and PTES discharging mode. To minimize plant complexity and avoid the need for additional piping and valves, during discharge the cycle working fluid should pass through the same sequence of components in both CSP-mode and PTES discharging mode, and a heat engine layout that achieves this is shown in Fig. 4.

The CSP-mode heat engine operates at different operating conditions to the PTES-mode heat engine: since no cold storage is available, heat is rejected to the environment, and as a result the discharging compressor inlet temperature is hotter than in PTES-mode. Increasing the compressor inlet temperature requires the off-design performance of the turbomachinery to be considered [37–39]. Since this is a closed cycle, the pressure ratios of the compressor and turbine must be roughly equal. By varying the system pressure it is possible to find a solution whereby the compressor inlet temperature is increased while the pressure ratios are matched [37–39]. This off-design operation compromises the CSP-mode efficiency to a small extent.

Another feature of the CSP-mode heat engine is the constraint that the working fluid follows the same sequence of components as in PTES-mode. As a result, after the turbine, the working fluid enters the ‘cold’

PFBHX which now operates as a recuperator: cool particles leaving the hot PFBHX are transferred to the cold PFBHX where they are heated by the hot turbine exhaust, before being heated to maximum temperature in the solar receiver. This arrangement requires an extra particle lift to move particles from the hot PFBHX to the cold PFBHX. The particles now provide recuperation from one side of the cycle to the other, which reduces the temperature range over which solar heat is added to the cycle, therefore improving the heat engine efficiency.

The performance of the system can therefore be defined in terms of the round-trip efficiency η_{RT} of the PTES device (equation (1)) and the heat engine efficiency of the CSP power cycle η_{HE} , where

$$\eta_{HE} = \frac{W_{out}^{dis}}{Q_{solar}} \tag{3}$$

3. Modelling methods

A simple thermodynamic model of the above systems is described here. This model is sufficient to gather initial estimates of performance and explore sensitivity to various parameters. More detailed models (including transient models and off-design models) are currently being developed. The main components to model are the turbomachines and the pressurized fluidized bed heat exchangers (PFBHX), but other components such as the motors, generators, and heat rejection equipment are also considered, and nominal values are shown in Table 1. The working fluid (gas) properties are calculated using CoolProp [40] – although nitrogen is often modelled as an ideal gas, heat capacity variations over the range of operating temperatures do have an appreciable impact on performance, and are therefore included. The particles are assumed to be uniformly sized and shaped (on average) and are also modelled with a temperature-invariant (average) heat capacity.

Compressors and turbines are turbomachines that are modelled with a polytropic efficiency η_p . For a compression process, the infinitesimal specific work input is given by $dw = dp/(\eta_p \rho)$, which for perfect gases leads to

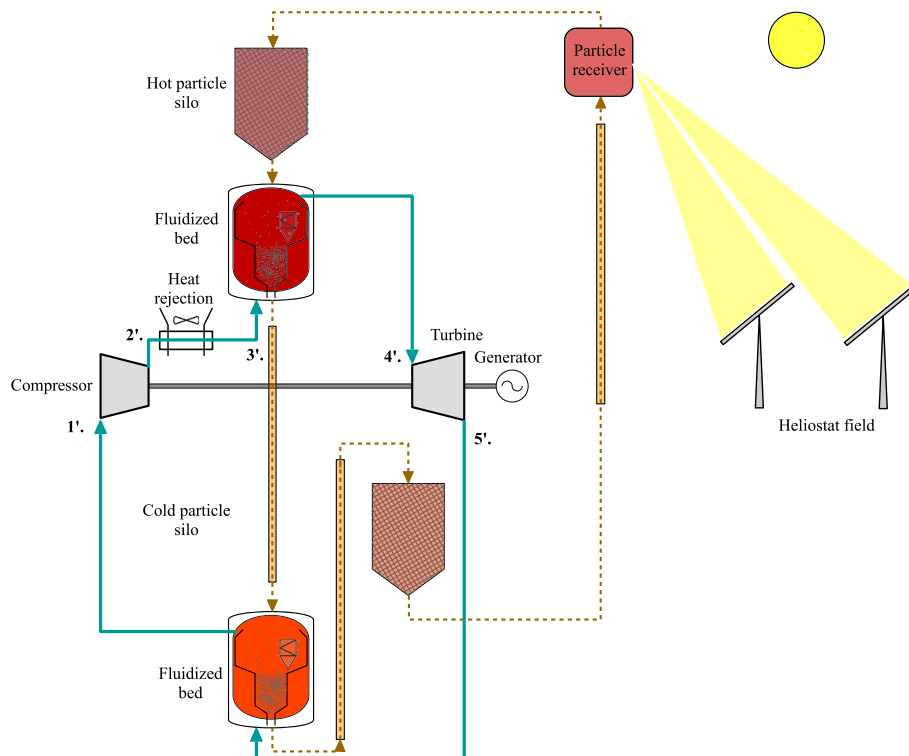


Fig. 4. Schematic illustrating a solar thermal heat engine using the same components as the Pumped Thermal Energy Storage system.

Table 1
Nominal design inputs used for calculations, unless otherwise stated.

Parameter	Value
Gas cycle working fluid	Nitrogen
Turbomachinery polytropic efficiency	% 90
Motor-generator efficiency	% 98
Fan efficiency	% 70
Hot HX approach temperature	K 10
Cold HX approach temperature	K 10
Heat rejection approach temperature	K 4
Hot HX pressure loss	% 2.5
Cold HX pressure loss	% 2.5
Heat rejection pressure loss	% 1.0
Charge compressor inlet pressure	bar 5
Steam cycle pump efficiency	% 70
Steam cycle turbine efficiency	% 80
Steam cycle boiler approach temperature	K 25
Steam cycle boiler pressure loss	% 5
Steam cycle maximum pressure	bar 100
Steam cycle maximum temperature	K 873

$$\frac{T_2}{T_1} = \left(\frac{p_2}{p_1}\right)^{\frac{\gamma-1}{\gamma}} \quad (4)$$

A similar expression can be found for expansion processes. Due to the variation in heat capacity of the working fluid, Equation (4) is integrated over the temperature range of the compressor (or expander) and the fluid properties are calculated using CoolProp [40]. It is assumed that the compressor and expander are on the same shaft, and are therefore driven by a motor during charge and turn a generator during discharge. The motor and generator have an efficiency – e.g. the mechanical work into the cycle during charge is less than the electrical work provided to the motor.

The PFBHXs are simply modelled by assuming that there is a fixed temperature difference ΔT between the gas and the particles. For example, during charge in the hot PFBHX, the gas is at T_2 and is cooled down to T_3 , while the hot particles are initially at $T_3 - \Delta T$ and are heated up to $T_2 - \Delta T$. There is also a pressure loss in the PFBHX which is defined in terms of a fractional pressure loss $f_p = \Delta p/p_{in}$.

Air fans are also required to move air through the heat rejection equipment, and the work input to these fans is calculated using a polytropic efficiency combined with a pressure ratio $p_2/p_1 = 1/(1 - f_p)$, where f_p is the fractional pressure loss on the air side of the heat rejection equipment.

It is possible to evaluate the performance of the charge and discharge cycle with these assumptions, along with specifying fluid conditions. Typically, the charge compressor inlet temperature T_1 and pressure p_1 are specified, along with the outlet temperature T_2 . The model then calculates the performance of each component sequentially until the cycle is closed. The particle temperatures at the end of charge are used as the starting point for the discharge cycle. The discharge cycle pressure ratio is found by the requirement that the cold particles are returned to their initial temperature. As shown in Fig. 2 this typically means that the discharging pressure ratio is larger than the charging pressure ratio.

Once the temperatures and pressures around the charge and discharge cycle have been evaluated, the specific work input and output is calculated as well as the round-trip efficiency defined in Equation (1).

Finally, the user also specifies the discharging power output \dot{W}_{out}^{dis} and the duration of the charging τ_{chg} and discharging processes τ_{dis} . This information is used to find the size of the components. Throughout this section, it is assumed that charge and discharge have equal durations $\tau_{chg} = \tau_{dis}$. Thus, the charging power input is given by $\dot{W}_{in}^{chg} = \dot{W}_{out}^{dis}/\eta_{RT}$, and the gas mass flow rate is $\dot{m} = \dot{W}_{out}^{dis}/w_{out}^{dis}$ which is equal during charge and discharge. This mass flow rate can then be used to find the work input/output to each compressor/turbine, and therefore size those devices.

For the Solar Top-Up hybrid cycle, a subcritical steam turbine cycle is modelled. The steam cycle comprises a pump, boiler, turbine, and heat rejection equipment. These components are also modelled using polytropic efficiencies, approach temperatures, and pressure loss factors, as detailed in Table 1, and steam properties are calculated using CoolProp.

4. PTES with solar thermal input

4.1. Solar Top-Up cycle

An illustrative temperature-entropy diagram of a solar top-up cycle is shown in Fig. 5. The heat pump heats particles to a temperature of $T_2 = 750K$ which is similar to the outlet temperature of gas compressors in simple gas turbine cycles. The particle temperature is then upgraded to $T_{solar} = 1100K$ using solar heat. This particular example has a second-law round-trip efficiency of $\eta_{RT,2} = 61.7\%$, and specific work output of 301 kJ/kg, 75 % of which is produced by the gas cycle, as shown in Table 2. For comparison, this nominal design is compared to two stand-alone PTES systems, with maximum temperatures of $T_2 = 750 K$ and $T_2 = 1100 K$. A stand-alone PTES with $T_2 = 750 K$ has a notably lower roundtrip efficiency (40.1 %) and specific work output (88 kJ/kg) than the Solar Top-Up cycle. Better performance is achieved by increasing the heat pump temperature to $T_2 = 1100 K$, in which case $\eta_{RT} = 60.8\%$. This value is very similar to the Solar Top-Up cycle (it should be noted that neither of these cycles have been optimized) and illustrates that the less complex PTES could be preferable to the hybrid cycle. However, it is notable that the Solar Top-Up cycle generates significantly more work than either of the PTES systems by virtue of the solar heat addition and bottoming steam cycle. This may help reduce the capital cost per unit power output. Therefore, the hybrid Solar Top-Up cycle is a viable option when power output is a priority, or when solar heat can generate higher temperatures than available compression technology.

Results in Table 2 indicate that the majority of the power delivered by the hybrid system comes from the Brayton cycle, but that the steam cycle provides an important contribution – about 25–50 % of the total. Including the steam cycle increases $\eta_{RT,2}$ from 46.1 % to 61.7 %. Without the steam cycle, the system would consume more power during charge

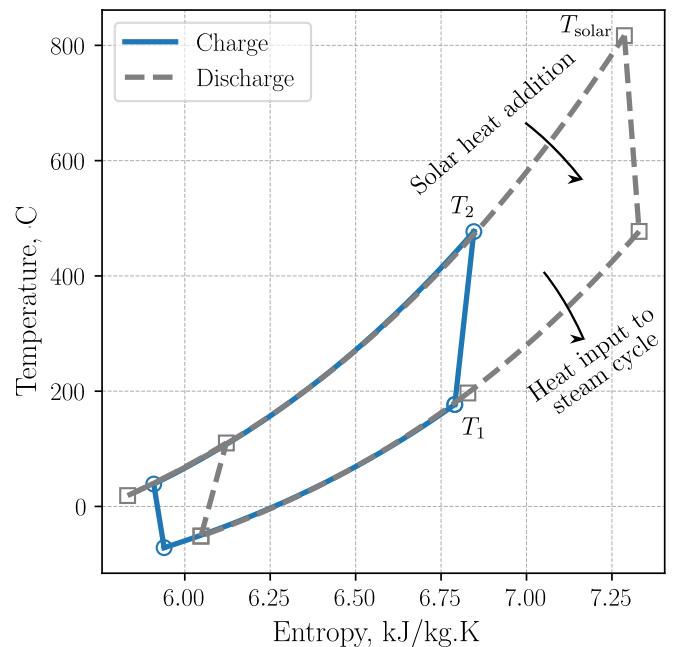


Fig. 5. Temperature-entropy diagram for a hybrid PTES-CSP system. The PTES heat pump has a maximum temperature T_2 of 750 K and a compressor inlet temperature T_1 of 450 K. The solar heat is added up to $T_{solar} = 1100 K$. The waste heat during discharge is used to power a bottoming steam cycle.

Table 2
Comparison of a Solar Top-Up cycle with two PTES systems.

		Solar top-up	PTES $T_2 = 750$ K	PTES $T_2 = 1100$ K
T_1	K	450	450	800
T_2	K	750	750	1100
T_{solar}	K	1100	–	–
$\eta_{RT,2}$	%	61.7	40.7	60.8
$\eta_{RT,2}$ without steam cycle		46.1	–	–
Gas cycle specific work	kJ/kg	225.1	88.1	219.3
Steam cycle specific work	kJ/kg	76.2	–	–
Total specific work	kJ/kg	301.3	88.1	219.3

than it produces during discharge. Although this is normal for pure electricity storage devices, it does not represent an effective use of solar energy. Therefore, the bottoming steam cycle is necessary to improve the prospects of this system.

The round-trip efficiency depends on numerous design parameters such as the pressure ratio, maximum heat pump temperature T_2 , and solar heat addition temperature T_{solar} . Fig. 6 and Fig. 7 show the second-law round-trip efficiency and specific work output for a range of pressure ratios and solar temperatures. Two values of T_2 are considered: $T_2 = 750\text{K}$ represents cycles that could be developed by modifying available gas compressors, and $T_2 = 1100\text{K}$ represents cycles that would require specific development of high-temperature compressors. For round-trip efficiency, an optimal pressure ratio exists and arises for the same reasons as in stand-alone PTES: a trade-off between exergy losses in the heat exchangers and turbomachinery [27]. The specific work output increases with pressure ratio, so a trade-off exists between maximizing efficiency and power output, as is typical with gas cycles. Increasing the solar temperature intuitively leads to higher round-trip efficiencies, although there are diminishing returns as the temperature becomes very high. Particle receivers are being developed to produce temperatures of 1100 K and a solar top-up cycle using such a receiver reaches $\eta_{RT,2} > 60\%$. Developing solar receivers that can generate higher temperatures can increase the round-trip efficiency further. For example, Fig. 6b shows the impact of solar temperatures up to 1400 K for a system with $T_2 = 1100\text{K}$ in which case efficiencies over 70 % can be achieved.

A similar hybrid system was proposed by Petrollese et al. in Ref. [10] which used argon working fluid and packed bed TES. This design did not

make use of a bottoming steam cycle but recorded $\eta_{RT,2} = 60.4\%$ for a maximum solar temperature of 1000 K, $T_2 = 823\text{K}$, and a pressure ratio of 5.2. The efficiency of a similar design point on Fig. 6a is $\eta_{RT,2} = 59\%$, and without the bottoming steam cycle $\eta_{RT,2}$ is 45.8 %. This highlights the importance of the bottoming cycle for improving the efficiency. The value without the bottoming cycle is notably lower than the corresponding design in Ref. [10] and this is attributable to several factors, mainly the use of packed-bed TES which achieves small approach temperatures. Running the model described in Section 3 with updated inputs ($\Delta T = 1\text{K}$, argon working fluid, $T_1 = 400\text{K}$, $T_2 = 823\text{K}$, $T_{\text{solar}} = 1000\text{K}$), leads to $\eta_{RT,2} = 57.5\%$ and 63.9%, without and with the steam bottoming cycle, respectively. These results are more similar to those in Ref [10], and discrepancies may be due to differences in the cycle conditions and assumptions about motor-generator efficiency. (Ref [10] does not mention this efficiency term which reduces $\eta_{RT,2}$ by several percentage points). This comparison is illustrative of potential improvements that can be made to the design presented in this work. Future work should establish whether PFBHX approach temperatures below 10 K are possible, as well as exploring the potential benefits of argon working fluid.

These results are all generated assuming the PFBHXs have approach temperatures of 10 K and pressure losses of 2.5 %. Reducing these sources of loss can also significantly increase the performance of the hybrid system.

4.2. Dual-Mode hybrid cycle

The Dual-Mode hybrid cycle uses the same set of components (turbomachinery, thermal storage, and heat exchangers) to operate in two different modes (1) Pumped Thermal Energy Storage (PTES) mode (2) CSP mode. In PTES-mode, the system operates the same as a stand-alone PTES as described in Section 2.1: electricity input drives a heat pump to create hot and cold particle storage. Later a heat engine runs between the two thermal reservoirs.

In CSP-mode, solar thermal energy is used to charge the hot storage to the same temperature as the heat pump ($T_{\text{solar}} = T_2$) but sub-ambient cold storage is not created. As a result, the discharge cycle differs slightly from the PTES-mode discharge cycle, as the compressor inlet temperature is warmer and particles are used to recuperate heat within the cycle. The particles and working fluid pass through the components in the same sequence as in PTES-mode. Unlike PTES-mode, where there are two sets of particles associated with either the hot storage or cold storage, in CSP-mode the particles travel in a continuous loop. The particle temperatures for PTES-mode and CSP-mode are compared in Table 3.

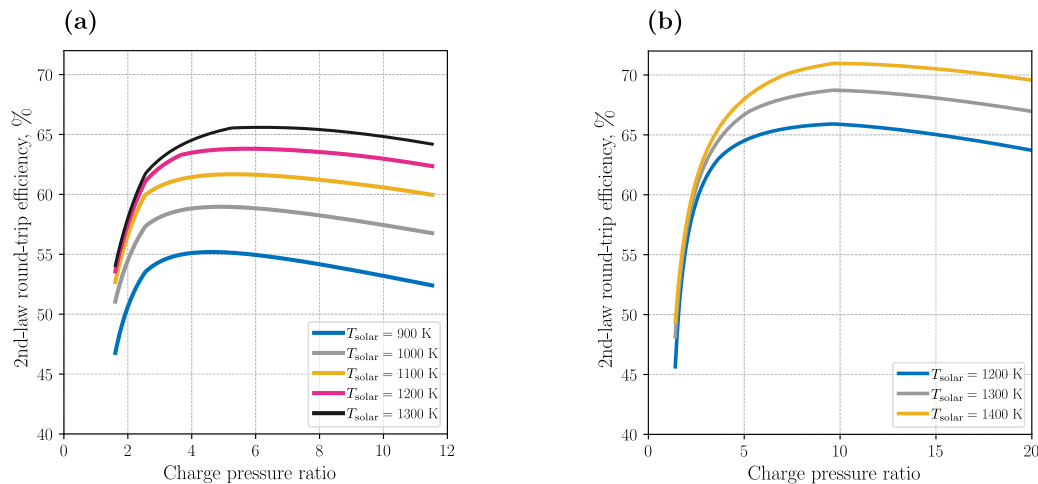


Fig. 6. Round-trip efficiency of a solar top up system as a function of pressure ratio and solar heat addition temperature. (a) Maximum PTES temperature is 750 K (b) Maximum PTES temperature is 1100 K.

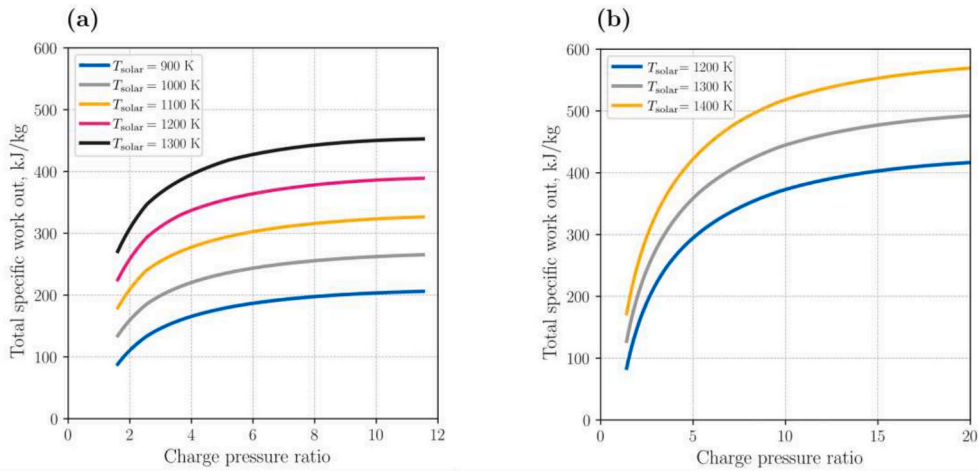


Fig. 7. Total specific work output of a solar top up system as a function of pressure ratio and solar heat addition temperature. (a) Maximum PTES temperature is 750 K (b) Maximum PTES temperature is 1100 K.

Table 3

Comparison of temperatures around the Dual-Mode cycle in PTES-mode and CSP-mode.

		PTES-mode	CSP-mode
T ₁ '	°C	-17.7	39.0
T ₂ '	°C	110.4	216.2
T ₃ '	°C	19.0	19.0
T ₄ '	°C	807.0	817.0
T ₅ '	°C	547.0	39.0
T _{in, hot PFBHX}	°C	817.0	827.0
T _{out, hot PFBHX}	°C	29.0	29.0
T _{in, cold PFBHX}	°C	-27.7	29.0
T _{out, cold PFBHX}	°C	537.0	526.1
T _{solar}	°C	-	827.0
Compressor inlet pressure	bar	5.0	4.1
Expander pressure ratio		3.3	3.6
Efficiency	%	59.8	39.1
Specific work output	kJ/kg	164.3	136.4

The particles initially leave the particle receiver having been heated to T_{solar}, and are then cooled to just above ambient temperature in the hot PFBHX, thereby transferring their heat to the power cycle. The particles

are then transferred to the cold PFBHX where they are heated by the hot gas from the turbine exhaust, see Fig. 4. This recuperates heat from the thermal cycle which helps to improve its efficiency. The particles then return to the particle receiver to be heated by solar energy.

In CSP-mode the compressor inlet temperature is close to ambient temperature due to the lack of cold storage, and is therefore considerably warmer than the inlet temperature during PTES-mode (which is at sub-ambient temperatures), as illustrated in Table 3 and the temperature-entropy diagrams of Fig. 8. It is assumed that the components are designed for PTES-mode conditions. Therefore, in CSP-mode the compressor operates at off-design conditions. It is also assumed that the compressor and turbine are on the same shaft and rotate at a constant speed, and that the closed gas cycle requires compressor and turbine pressure ratios to be roughly equal. The hot compressor inlet therefore requires careful management of the CSP-mode power cycle. Previous work in Ref. [41] described how these operating constraints can be met while varying the compressor inlet temperature. A strategy known as ‘inventory control’ is employed whereby the mass of gas in the cycle is varied – along with the compressor inlet pressure. These two parameters are varied to keep the volumetric flow through the turbomachines roughly constant, which keeps the turbomachine pressure ratio and efficiency close to the design value. As described in Ref. [41], it is possible to adjust the compressor inlet pressure and find an operating

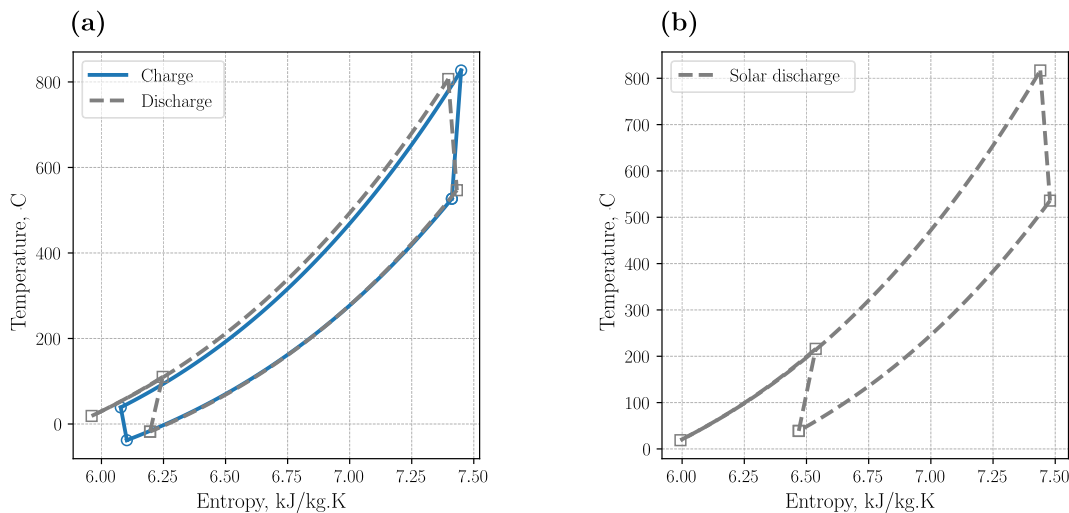


Fig. 8. Temperature-entropy diagrams of the dual-mode hybrid cycle. (a) PTES-mode. (b) CSP-mode.

point with matched pressure ratios in the compressor and turbine. For the example in Table 3, the compressor inlet pressure reduces and the cycle pressure ratio increases to accommodate the increased compressor inlet temperature. In this work, the design pressure ratio is set by PTES-mode, while an off-design pressure ratio is obtained in CSP-mode.

PTES-mode and CSP-mode achieve optimal performance at different operating conditions, and this therefore requires a trade-off between the two modes. For example, Fig. 9 illustrates the trade-off between cycle efficiency and specific work output, with the PTES charge pressure ratio being varied along the curves. (The PTES pressure ratio is effectively the design pressure ratio, and the CSP-mode performance is then calculated having found the off-design pressure ratio that enables operation). The figure shows that the efficiency and specific work are optimized at different charge pressure ratios. Furthermore, the optimal PTES-mode round-trip efficiency occurs at a different pressure ratio to the optimal CSP-mode heat engine efficiency – and this is also true for the specific work output.

Choosing a design point will depend on the priorities of individual designs. But it is notable that curves for CSP-mode are relatively steep: choosing a pressure ratio slightly different to the optimal value leads to a low efficiency and power output. On the other hand, PTES-mode curves have large flat sections which suggests that small reductions in PTES-mode performance should be made to achieve reasonable CSP-mode performance. One example is illustrated in Fig. 9: a design pressure ratio is chosen to provide the best compromise in efficiency and work output for CSP-mode, as shown by the square markers. The corresponding PTES-mode performance for that pressure ratio is shown by circle markers. (This ‘optimal’ pressure ratio is 2.2 for $T_2 = 750$ K and 2.9 for $T_2 = 1100$ K). PTES-mode performance could be improved by increasing the pressure ratio further, but this would lead to a rapid reduction in CSP-mode performance due to the steep curve shapes.

CSP-mode performance is improved by modifying the cycle design. For instance, multiple intercooled discharge compressions reduce the total compression work and therefore increase the efficiency and power output, as explored in Ref [41]. However, this design increases

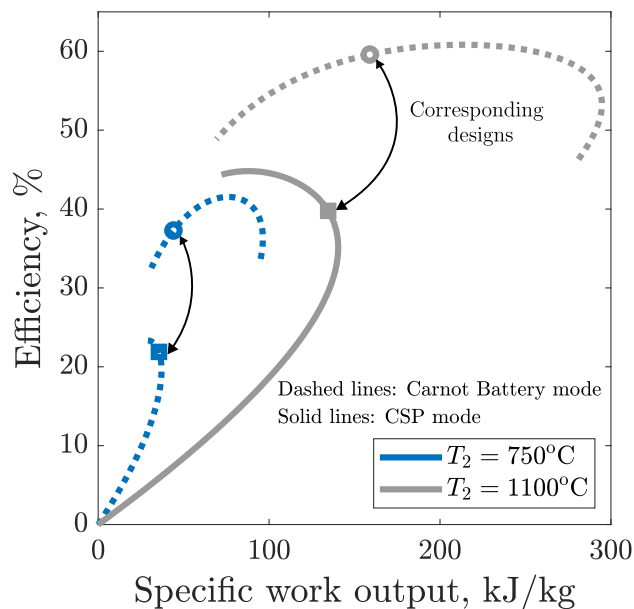


Fig. 9. Efficiency and work output of the Dual-Mode system for two values of T_2 . T_{solar} is equal to T_2 . Pressure ratio is varied along the curves. Efficiency is heat engine efficiency for CSP-mode and round-trip efficiency for PTES-mode. An optimal pressure ratio is chosen for the CSP-mode (square markers), and the corresponding PTES-mode performance is indicated at that pressure ratio. Dashed lines show the PTES round-trip efficiency. Solid lines show the CSP heat engine efficiency.

complexity and cost, and reduces PTES-mode performance. Another design change is to allow the particle receiver to heat the particles to higher temperatures than the heat pump – i.e. $T_{solar} > T_2$. This solution is feasible because the storage particles can be operated over a large temperature range. In this design, the CSP-mode turbine has a hotter inlet temperature (T_{solar}) than the design inlet temperature, T_2 . The inventory control method is used to find a cycle pressure that ensures the compressor and turbine pressure ratios are matched.

The impact of increasing T_2 on system performance is shown in Fig. 10. For each value of T_{solar} , T_2 is held constant at either 750 K or 1100 K, while the design pressure ratio is varied to optimize the CSP-mode performance as described above. Therefore, in this analysis PTES-mode performance also varies as a function of this chosen pressure ratio. In this case, Fig. 10 shows that increasing T_{solar} improves the efficiency and specific work output of both CSP-mode and PTES-mode, although PTES-mode results do not vary substantially.

Operating the turbomachinery at off-design conditions in PTES-mode may reduce system lifetime and increase maintenance costs. Fig. 11a shows the design pressure ratio in dashed lines for each value of T_{solar} . The off-design pressure ratio for CSP-mode is shown in solid lines, and it can be seen that increasing T_{solar} leads to a larger difference between the design and off-design values. The turbomachinery efficiency is also compromised by off-design operation, and off-design values are provided in Fig. 11b (the design efficiency is 90 %). Compressor efficiency is the most severely affected and reduces as T_{solar} increases. The turbine efficiency shows a more complex trend.

5. Outlook and conclusions

Pumped Thermal Energy Storage (PTES) is being developed for long duration energy storage, and various thermal storage media and power cycles have been considered so far. A developing suite of concepts integrate PTES with other thermal sources and sinks, which increases the range of services that can be delivered. In this article, two concepts that integrate a PTES with Concentrating Solar Power (CSP) are described and evaluated. These concepts are characterized by the use of silica particles for thermal energy storage. These particles can be operated over a wide range of temperatures and have low material costs. Heat is transferred between the particles and power cycle fluid via direct-contact heat exchangers that enable large heat transfer areas and highly effective heat transfer. Previous analysis found that particle-based PTES can achieve higher round-trip efficiencies and specific work output and lower Levelized Cost of Storage (LCOS) than due to higher potential temperatures and lower cost of storage and heat exchangers [27].

Two concepts for hybridizing a PTES with CSP are introduced in this article. Hybrid systems share components with the objective of reducing costs, enhancing performance, and/or providing a greater range of services and therefore greater value.

In the ‘Solar Top-Up’ concept, solar heat is used to upgrade the maximum temperature delivered by the charging heat pump. This enables the maximum temperature of the PTES to be increased without requiring the design of a novel heat pump compressor to reach those high temperatures. This design ‘unbalances’ the thermal storage, as the capacity of the hot storage is increased while the cold storage capacity is not increased. To exploit the abundance of hot thermal energy, a bottoming steam cycle is used during discharge. It is found that this hybrid system achieves a second-law round-trip efficiency comparable with a stand-alone PTES operating at the same maximum temperature, which is consistent with the results of Ref. [6]. However, the hybrid system has a much higher specific work output due to the solar heat addition. It is also notable that while the steam turbine work output is small compared to the Brayton cycle, it is an essential component to facilitate reasonable efficiencies and high work outputs.

The Solar Top-Up system places several constraints on operation: the charging heat pump must operate before the solar heat input, although it

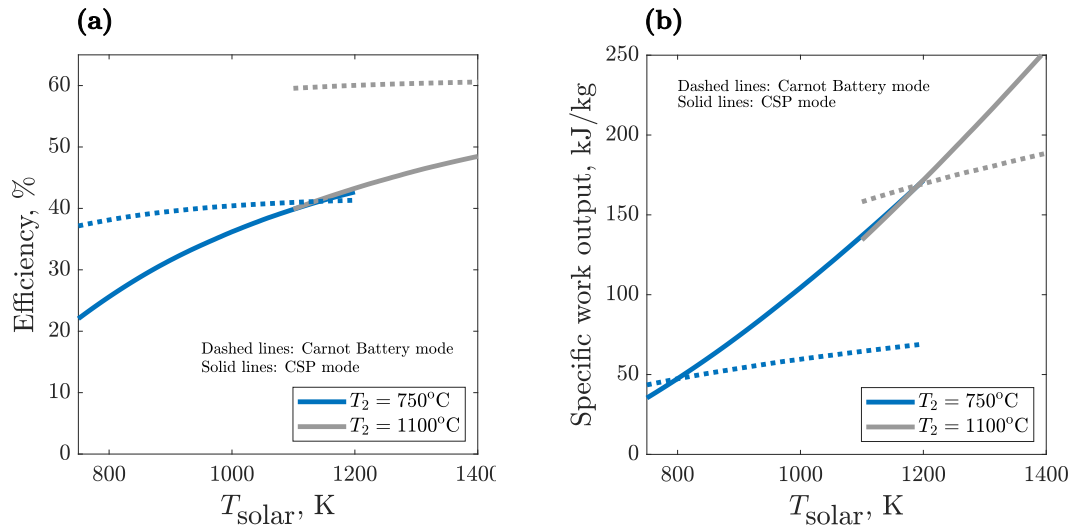


Fig. 10. Efficiency and work output as a function of T_{solar} . For each T_{solar} an optimal pressure ratio is chosen, and this affects the performance of the PTES system, which is also shown. (a) Efficiency (b) Specific work output.

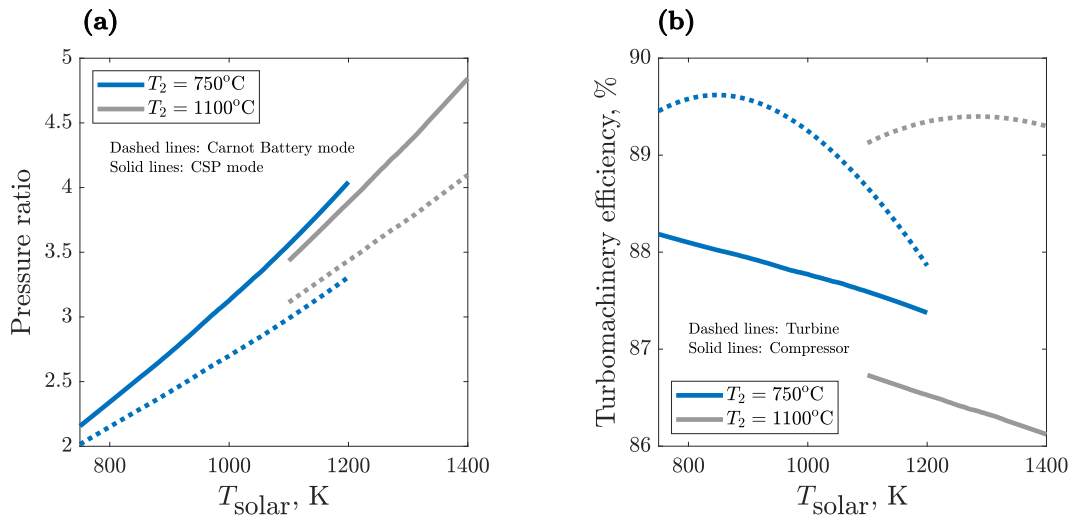


Fig. 11. Pressure ratio and turbomachinery efficiency as a function of T_{solar} . (a) Pressure ratio (b) Turbomachinery efficiency.

is possible for these systems to operate simultaneously or sequentially. The discharging cycle can only run if both the heat pump and solar charge have operated, which may provide challenges during periods of low solar availability. Furthermore, the potential solar heat addition is constrained by the availability of partially-heated particles – i.e. reduced operation of the heat pump limits the subsequent addition of solar thermal energy. The discharging Brayton cycle and discharging bottoming steam cycle can run simultaneously or at separate times (if intermediate storage is included), but the Brayton cycle must run before the steam cycle. These characteristics would be beneficial in an electrical grid scenario with large quantities of solar energy where favorable electricity prices are likely to coincide with solar availability: this means both the heat pump and solar charge can operate simultaneously. It is also notable that the hybrid system can discharge at high power outputs (compared to stand-alone PTES), which is useful in scenarios where there are short duration periods where the grid requires large quantities of energy.

The second hybrid system is a “Dual-Mode” device operates as either a conventional PTES or a CSP electricity generation system. This hybrid system uses the same turbomachinery, heat exchangers, and storage systems during the discharge of PTES or CSP, thereby reducing system

costs compared to two stand-alone systems. However, the discharging CSP system does not have cold storage, therefore the discharging compressor operates away from the design point set by the PTES, so inventory control is used to manage the off-design operating point.

Choosing a design pressure ratio is challenging because the optimal efficiency and work output occur at different values, and also differ for PTES-mode and CSP-mode. CSP-mode performance is more sensitive to the pressure ratio than PTES-mode, so a method of choosing a pressure ratio based on CSP-mode is suggested here. CSP-mode efficiency and work output can be significantly improved by allowing the particle receiver to operate at higher temperatures. Depending on how the pressure ratio is chosen, this has a small (beneficial) impact on PTES-mode. Designs are found that achieve PTES round-trip efficiencies > 60 %, CSP heat engine efficiencies > 40 %, and specific work outputs > 150 kJ/kg (for both cycles), when the particle receiver temperature is > 1200 K and maximum heat pump temperature is 1100 K. However, this does require the turbomachinery to operate at more extreme off-design conditions, potentially reducing lifetime and increasing maintenance costs.

The Dual-Mode system places several constraints on system operation. The charging heat pump and charging solar heat addition can occur

simultaneously or separately, although running simultaneously will require suitable capacity on the particle conveyance system and storage silos. During discharge, there is one set of turbomachinery and heat exchangers available shared between the PTES and CSP, so the solar energy and heat pump energy must be discharged at separate times. These characteristics may be suitable for an electrical grid where charging opportunities are brief but discharging opportunities are long – e.g. a solar dominated grid where a large quantity of energy has to be stored in a short period of time (early afternoon), but this energy is then discharged over a longer period (overnight). The Dual-Mode system can charge the PTES and CSP simultaneously which effectively increases the charging rate. Discharging the PTES and CSP sequentially means the discharging duration is relatively long. Previous research has suggested that PTES charging durations are relatively short compared to discharging durations [42]. Operating a standalone PTES with a charging duration half the discharge duration is challenging because the charge power rating would be three-to-four times greater than the discharging power rating which has substantial implications on the system cost and the design the heat exchangers, motors and generators. The Dual-Mode system can also mitigate against seasonal variations in solar availability: for example, in the winter the system will predominantly operate as a PTES device and mean that all the components are being used to a high capacity factor.

Future work on particle-based hybrid PTES-CSP cycles should evaluate the costs and value of such systems, and compare these to alternative technologies. Particular attention should be paid to part-load operation and to the actual charge–discharge schedules that real operation would require.

CRediT authorship contribution statement

Joshua McTigue: Writing – original draft, Visualization, Methodology, Investigation, Formal analysis, Data curation, Conceptualization. **Zhiwen Ma:** Writing – review & editing, Supervision, Project administration, Funding acquisition.

Declaration of Competing Interest

The authors declare that they have no known competing financial interests or personal relationships that could have appeared to influence the work reported in this paper.

Acknowledgements

This work was authored in part by the National Renewable Energy Laboratory, operated by Alliance for Sustainable Energy, LLC, for the U.S. Department of Energy (DOE) under Contract No. DE-AC36-08GO28308. Funding was provided by U.S. Department of Energy Office of Energy Efficiency and Renewable Energy (EERE) Solar Energy Technologies Office (SETO). The views expressed in the article do not necessarily represent the views of the DOE or the U.S. Government. The U.S. Government retains and the publisher, by accepting the article for publication, acknowledges that the U.S. Government retains a nonexclusive, paid-up, irrevocable, worldwide license to publish or reproduce the published form of this work, or allow others to do so, for U.S. Government purposes.

References

- [1] U.S. Department of Energy, Pathways to Commercial Liftoff: Long Duration Energy Storage, 2023.
- [2] Andy Colthorpe, Germany plans long-duration energy storage auctions for 2025 and 2026, Energy Storage News (2024). <https://www.energy-storage.news/germany-plans-long-duration-energy-storage-auctions-for-2025-and-2026/> (accessed November 3, 2024).
- [3] California Public Utilities Commission, Decision Determining Need for Centralized Procurement of Long Lead-Time Resources, 2024. <https://docs.cpuc.ca.gov/PublishedDocs/Efile/G000/M536/K273/536273174.PDF>.
- [4] Ivan Shumkov, Liquid air energy storage specialist Highview Power raises GBP 300m, Renewables Now (2024). <https://renewablesnow.com/news/liquid-air-energy-storage-specialist-highview-power-raises-gbp-300m-860598/> (accessed November 3, 2024).
- [5] Long-Duration Energy Storage, Office of Clean Energy Demonstrations (2024). <https://www.energy.gov/oced/long-duration-energy-storage> (accessed November 3, 2024).
- [6] J.D. McTigue, P. Farres-Antunez, C.N. Markides, A.J. White, Integration of heat pumps with solar thermal systems for energy storage, in: Encyclopedia of Energy Storage, Elsevier, 2022. doi: 10.1016/B978-0-12-819723-3.00131-1.
- [7] D. Fiaschi, G. Manfrida, K. Petela, L. Talluri, Thermo-Electric Energy Storage with Solar Heat Integration: Exergy and Exergo-Economic Analysis, Energies (basel) 12 (2019) 648, <https://doi.org/10.3390/en12040648>.
- [8] A. Benato, Performance and cost evaluation of an innovative Pumped Thermal Electricity Storage power system, Energy (2017), <https://doi.org/10.1016/j.energy.2017.07.066>.
- [9] L.X. Chen, P. Hu, M.N. Xie, F.X. Wang, Thermodynamic analysis of a high temperature pumped thermal electricity storage (HT-PTES) integrated with a parallel organic Rankine cycle (ORC), Energy Convers. Manag. 177 (2018) 150–160, <https://doi.org/10.1016/j.enconman.2018.09.049>.
- [10] M. Petrollese, M. Cascetta, V. Tola, D. Cocco, G. Cau, Pumped thermal energy storage systems integrated with a concentrating solar power section: Conceptual design and performance evaluation, Energy (2022) 123516, <https://doi.org/10.1016/j.energy.2022.123516>.
- [11] P. Farrés-Antúnez, Modelling and development of thermo-mechanical energy storage, University of Cambridge (2018), <https://doi.org/10.17863/CAM.38056>.
- [12] M. Cascetta, F. Licheri, R.P. Merchan, M. Petrollese, Operating performance of a Joule-Brayton pumped thermal energy storage system integrated with a concentrated solar power plant, J Energy Storage 73 (2023), <https://doi.org/10.1016/j.est.2023.108865>.
- [13] T. Neises, Steady-state off-design modeling of the supercritical carbon dioxide recompression cycle for concentrating solar power applications with two-tank sensible-heat storage, Sol. Energy 212 (2020) 19–33, <https://doi.org/10.1016/j.solener.2020.10.041>.
- [14] J.D. McTigue, P. Farres-Antunez, T. Neises, A. White, Supercritical CO₂ Heat Pumps and Power Cycles for Concentrating Solar Power, SolarPACES (2020). <https://www.nrel.gov/docs/fy21osti/77955.pdf>.
- [15] A.J. Subires, A. Rovira, M. Muñoz, Proposal and study of a pumped thermal energy storage to improve the economic results of a concentrated solar power that works with a hybrid rankine–brayton propane cycle, Energies (basel) 17 (2024), <https://doi.org/10.3390/en17092005>.
- [16] Z. Ma, R. Zhang, F. Sawaged, Design of a Particle-Based Thermal Energy Storage for a Concentrating Solar Power System, in: Proceedings of the ASME 2017 11th International Conference on Energy Sustainability, Charlotte, North Carolina, 2018: pp. 1–8.
- [17] C.K. Ho, B.D. Iverson, Review of high-temperature central receiver designs for concentrating solar power, Renew. Sustain. Energy Rev. 29 (2014) 835–846, <https://doi.org/10.1016/j.rser.2013.08.099>.
- [18] Z. Ma, J. Martinek, C. Turchi, J. McTigue, J. Sment, C. Ho, Thermal energy storage for energy decarbonization, Annu. Rev. Heat Transfer (2022) 51–115.
- [19] Z. Ma, X. Wang, P. Davenport, J. Gifford, J. Martinek, J. Schirck, A. Morris, M. Lambert, R. Zhang, System and component development for long-duration energy storage, Appl. Therm. Eng. (2022) 119078, <https://doi.org/10.1016/j.applthermaleng.2022.119078>.
- [20] J. Gifford, Z. Ma, X. Wang, R. Braun, Computational fluid dynamic analysis of a novel particle-to-air fluidized-bed heat exchanger for particle-based thermal energy storage applications, J. Energy Storage 73 (2023), <https://doi.org/10.1016/j.est.2023.108635>.
- [21] Z. Ma, J. McTigue, J. Gifford, J. Hirsche, S.Y. Jeong, M.P. Shah, J. Martinek, System and Component Development of Particle-Based Pumped Thermal Energy Storage, in: Proceedings of the ASME 2024 18th International Conference on Energy Sustainability, Anaheim, California, 2024: pp. 1–8.
- [22] Z. Ma, Economic Long-Duration Electricity Storage by Using Low-Cost Thermal Energy Storage and High-Efficiency Power Cycle (ENDURING), 2023. www.nrel.gov/publications.
- [23] J.D. McTigue, Z. Ma, Pumped Thermal Energy Storage with Particle Silos and Fluidized Bed Heat Exchangers, in: SolarPACES 2022, Albuquerque, New Mexico, 2022.
- [24] J.D. McTigue, P. Farres-Antunez, C.N. Markides, A.J. White, Techno-economic analysis of recuperated Joule-Brayton pumped thermal energy storage, Energy Convers. Manage. 252 (2022) 115016, <https://doi.org/10.1016/j.enconman.2021.115016>.
- [25] R.B. Laughlin, Pumped thermal grid storage with heat exchange, J. Renew. Sustain. Energy 9 (2017), <https://doi.org/10.1063/1.4994054>.
- [26] J.D. McTigue, A.J. White, C.N. Markides, Parametric studies and optimisation of pumped thermal electricity storage, Appl. Energy 137 (2015), <https://doi.org/10.1016/j.apenergy.2014.08.039>.
- [27] J.D. McTigue, J. Hirsche, Z. Ma, Advancing pumped thermal energy storage performance and cost using silica storage media, Appl. Energy 387 (2025), <https://doi.org/10.1016/j.apenergy.2025.125567>.
- [28] M. Mehos, C. Turchi, J. Vidal, M. Wagner, Z. Ma, C. Ho, W. Kolb, C. Andracka, A. Kruiženga, Concentrating Solar Power Gen3 Demonstration Roadmap, NREL Technical Report, NREL/TP-5500-67464 (2017).
- [29] A.V. Olympios, J.D. McTigue, P. Farres-Antunez, A. Tafone, A. Romagnoli, Y. Li, Y. Ding, W.-D. Steinmann, L. Wang, H. Chen, C.N. Markides, Progress and

- prospects of thermo-mechanical energy storage—a critical review, *Prog. Energy* 3 (2021) 022001, <https://doi.org/10.1088/2516-1083/abdbba>.
- [30] Z. Ma, P. Davenport, J. Martinek, Particle-Based Thermal Energy Storage Systems, US Patent - No.: 11,181,326 B2, 2021.
- [31] A. White, G. Parks, C.N. Markides, Thermodynamic analysis of pumped thermal electricity storage, *Appl. Therm. Eng.* 53 (2013) 291–298, <https://doi.org/10.1016/j.applthermaleng.2012.03.030>.
- [32] J. McTigue, *Analysis and optimisation of thermal energy storage*, University of Cambridge, 2016.
- [33] J.D. McTigue, P. Farres-Antunez, C.N. Markides, A.J. White, Pumped thermal energy storage with liquid storage, *Encyclope. Energy Storage* (2021), <https://doi.org/10.1016/B978-0-12-819723-3.00054-8>.
- [34] J. McTigue, T. Neises, Off-design operation and performance of pumped thermal energy storage, *J. Energy Storage* 99 (2024), <https://doi.org/10.1016/j.est.2024.113355>.
- [35] A. Ghilardi, G.F. Frate, K. Kyprianidis, M. Tucci, L. Ferrari, Brayton pumped thermal energy storage: Optimal dispatchment in multi-energy districts, *Energy Convers. Manag.* 314 (2024), <https://doi.org/10.1016/j.enconman.2024.118650>.
- [36] R.B. Laughlin, Mass grid storage with reversible Brayton engines, in: K. Brun, T. Allison, R. Dennis (Eds.), *Thermal, Mechanical, and Hybrid Chemical Energy Storage Systems*, Elsevier, 2020.
- [37] A. Sciacovelli, Y. Li, H. Chen, Y. Wu, J. Wang, S. Garvey, Y. Ding, Dynamic simulation of Adiabatic Compressed Air Energy Storage (A-CAES) plant with integrated thermal storage – Link between components performance and plant performance, *Appl. Energy* 185 (2017) 16–28, <https://doi.org/10.1016/j.apenergy.2016.10.058>.
- [38] L.S. Dixon, C.A. Hall, *Fluid Mechanics and Thermodynamics of Turbomachinery*, Elsevier Science, 2010.
- [39] N. Zhang, R. Cai, Analytical solutions and typical characteristics of part-load performances of single shaft gas turbine and its cogeneration, *Energy Convers. Manag.* 43 (2002) 1323–1337, [https://doi.org/10.1016/S0196-8904\(02\)00018-3](https://doi.org/10.1016/S0196-8904(02)00018-3).
- [40] I.H. Bell, J. Wronski, S. Quoilin, V. Lemort, Pure and pseudo-pure fluid thermophysical property evaluation and the open-source thermophysical property library coolprop, *Ind. Eng. Chem. Res.* 53 (2014) 2498–2508, <https://doi.org/10.1021/ie4033999>.
- [41] J. McTigue, Z. Ma, A Dual-Mode Hybrid System Combining Solar Thermal with Pumped Thermal Energy Storage, in: *SolarPACES 2023*, Sydney, Australia, 2023: pp. 1–11.
- [42] J. Martinek, J. Jorgenson, J.D. McTigue, On the operational characteristics and economic value of pumped thermal energy storage, *J. Energy Storage* 52 (2022) 105005, <https://doi.org/10.1016/j.est.2022.105005>.